Marangoni flow around chemical fronts traveling in thin solution layers: influence of the liquid depth

Laurence Rongy · Anne De Wit

Abstract Surface-tension gradients, which can exist across autocatalytic chemical fronts propagating in thin layers of solution in contact with air, can induce capillary flows that are also called Marangoni flows. These flows in turn affect the spatio–temporal evolution of the concentration fields. This paper addresses the influence of the thickness of the solution layer on the chemo–hydrodynamic pattern resulting from such a coupling between autocatalytic reactions, diffusion and Marangoni effects, neglecting any buoyancy-driven effect. The system reaches an asymptotic dynamics characterized by a steady fluid vortex traveling at a constant speed with the front and deforming it. When the thickness of the fluid layer is increased, Marangoni effects are increasing, thus leading to a larger deformation of the chemical front, larger traveling speed, and more intense convection.

Keywords Chemical front · Marangoni convection · Steady fluid vortex

1 Introduction

When autocatalytic chemical fronts propagate in solution layers in the absence of any gel, diffusion is not the only transport process that can come into play. Convection driven by the concentration gradients across the front can affect the properties of the system as well. Such convection can be due to either density or surface-tension gradients triggered by the concentration gradients characterizing the evolution of the front. In the absence of contact with another fluid, only buoyancy effects can operate induced by density changes. Numerous experimental and theoretical works have analyzed the influence of buoyancy-driven convection on the evolution of autocatalytic fronts (see for instance [1–3] and refs therein). If the reactive solution is in contact with air, Marangoni flows due to the presence of surface-tension effects can come into play as well, thereby complicating the situation.

For example, wave fronts of different reactions such as the Belousov–Zhabotinsky reaction or the iodate–arsenous acid reaction have long been observed to propagate with non-constant velocities in Petri dishes open to the air (see refs [4–12]). Since those reactions are exothermic and involve variations of the solution density or

L. Rongy (✉) · A. De Wit
Nonlinear Physical Chemistry Unit, Center for Nonlinear Phenomena and Complex Systems, CP 231,
Université Libre de Bruxelles (U.L.B.), 1050 Brussels, Belgium
e-mail: lrongy@ulb.ac.be

A. De Wit
e-mail: adewit@ulb.ac.be

surface tension, convection resulting from both Marangoni and buoyancy effects may play an important role in these systems dynamics. Similarly, the origin of the precipitation patterns of BaSO$_4$ behind the traveling wave of the chlorite–thiourea–barium chloride reaction system was discussed qualitatively in terms of a coupling between thermocapillary (surface-tension-driven) and multicomponent (buoyancy-driven) convection [13–15]. Moreover, those chemical systems dynamics strongly depends on the layer depth since it affects the relative importance of Marangoni and buoyancy flows.

In this context, it is important to understand what is the influence of Marangoni effects on the propagation of chemical fronts in thin solution layers open to the air in the absence of any buoyancy-driven effects. To do so, we numerically integrate a two-dimensional (2D) reaction–diffusion–convection (RDC) model for the evolution of a chemical species involved in an autocatalytic process and affecting the surface tension of the liquid coupled to the incompressible Navier–Stokes equations for the velocity of the fluid. In dimensionless variables, the dynamics depend on two parameters: the Marangoni number M characterizes the strength of the coupling between the reaction–diffusion (RD) processes and the surface-tension-driven flows initiated at the surface of the layer. The second parameter is related to the geometry and is the solution thickness L_z. We have shown previously [16] that, for a fixed L_z, increasing the Marangoni number increases the influence of the flow leading to more deformed fronts traveling with a larger asymptotic convective speed. It is the objective of this article to analyze the influence of the thickness of the solution layer L_z on the deformation and speed-up of chemical fronts by capillary flows. We show that increasing L_z leads to more intense convection stretching the front and accelerating it in a first step. After this transient, the system reaches, whatever the value of L_z we have scanned, a steady asymptotic dynamics consisting of a steady vortex traveling with the front and deforming it. The speed of this reaction–diffusion–convection pattern is an increasing function of L_z.

The article is organized as follows. The model system is presented in Sect. 2 where we introduce the two relevant parameters of the model which are the Marangoni number M and the thickness of the solution layer L_z, respectively. In Sect. 3, we analyze the characteristics of the Marangoni-driven flow and the non-linear evolution of the system as a function of L_z keeping M constant. Conclusions are drawn in Sect. 4.

2 Model

Let us consider an isothermal planar chemical front propagating in a thin aqueous solution layer in contact with air (Fig. 1). The product of the reaction affects the surface tension of the solvent, so that the concentration gradient across the front triggers capillary flows. To simplify the theoretical description of the system, we assume no surface deformation and no evaporation, so that the air layer need not be considered here. We furthermore neglect any buoyancy-driven flow, considering the solution density as constant in space and time. In a two-dimensional system of length L'_x and height L'_z, the governing equations for this system are

$$\frac{\partial c}{\partial t} + \underline{v}.\nabla c = D\nabla^2 c + f(c), \tag{1}$$

$$\frac{\partial \underline{v}}{\partial t} + \underline{v}.\nabla \underline{v} = -\frac{1}{\rho_0}\underline{\nabla}p + \nu\nabla^2\underline{v} + \underline{g}, \tag{2}$$

$$\text{div } \underline{v} = 0. \tag{3}$$

Equations 2–3 are the incompressible Navier–Stokes equations describing the evolution of the 2D fluid velocity vector $\underline{v} = (u, w)$. The solution density ρ_0, the kinematic viscosity $\nu = \mu/\rho_0$, where μ is the dynamic viscosity, and the gravity acceleration $\underline{g} = (0, -g)$ are assumed constant and p denotes the pressure. These evolution equations for the flow are coupled to the reaction–diffusion–advection equation for the surface-active substance of concentration c, the molecular diffusion coefficient D being constant. As a typical autocatalytic kinetics capable of sustaining traveling fronts when coupled to diffusion, we take the simple one-variable cubic expression $f(c) = kc^2(a_0 - c)$, where a_0 is the initial reactant concentration and k is a kinetic constant.

Fig. 1 Sketch of the system
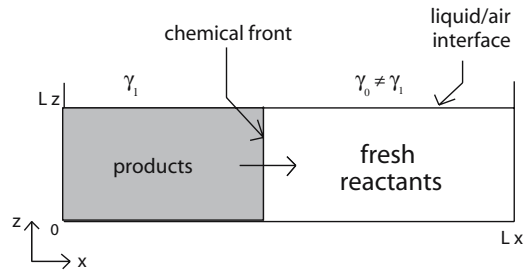
At each boundary of the domain, we require zero-flux boundary conditions for the chemical concentration c. The hydrodynamic boundary conditions are rigid side walls and a rigid bottom where no-slip conditions, $u = 0$ and $w = 0$, are applied for the flow velocity components. At the free surface, we have $w = 0$ and take

$$\mu \frac{\partial u}{\partial z} = \frac{\partial \gamma}{\partial x} \quad \text{at } z = L_z',$$ (4)

where γ is the surface tension of the solution. This expresses the fact that Marangoni effects drive a non-zero horizontal fluid velocity u when a horizontal surface-tension gradient exists [17].

To non-dimensionalize the problem, we scale the concentration by a_0, time by $\tau_c = 1/ka_0^2$, space by $L_c = \sqrt{D\tau_c}$, speed by $U_c = L_c/\tau_c = \sqrt{D/\tau_c}$, and pressure by $p_c = \rho_0 S_c D/\tau_c$, where the dimensionless parameter $S_c = \nu/D$ is the Schmidt number. We define in addition a new hydrostatic pressure gradient incorporating the constant dimensionless buoyancy term $\rho_0 L_c \underline{g}/p_c$. In terms of these RD scales and incorporating a linear dependence between the surface tension and the surfactant concentration,

$$\gamma = \gamma_o + \left(\frac{d\gamma}{dc}\right) c$$ (5)

with γ_0 being the surface tension of the reactant solution, we obtain the dimensionless evolution equations,

$$\frac{\partial c}{\partial t} + \underline{v}.\nabla c = \nabla^2 c + c^2(1-c),$$ (6)

$$\frac{\partial \underline{v}}{\partial t} + \underline{v}.\nabla \underline{v} = S_c(-\nabla p + \nabla^2 \underline{v}),$$ (7)

$$\text{div } \underline{v} = 0$$ (8)

with boundary conditions:

$$\frac{\partial c}{\partial x} = 0 = u = w \quad \text{at } x = 0, x = L_x,$$ (9)

$$\frac{\partial c}{\partial z} = 0 = u = w \quad \text{at } z = 0,$$ (10)

$$\frac{\partial c}{\partial z} = 0 = w \quad \text{at } z = L_z,$$ (11)

$$\frac{\partial u}{\partial z} = -M \frac{\partial c}{\partial x} \quad \text{at } z = L_z,$$ (12)

where $L_x = L_x'/L_c$ and $L_z = L_z'/L_c$ represent the dimensionless length and height of the layer, respectively. Condition (12) is the dimensionless form of Eq. 4 and introduces one of the dimensionless parameters of the problem, i.e., the solutal Marangoni number M:

$$M = \frac{-1}{\mu\sqrt{Dk}} \frac{d\gamma}{dc}.$$ (13)

We take here the Marangoni number as positive considering that the surface-active product decreases the surface tension behind the front. In terms of our RD scales, the chemical Marangoni number is inversely proportional to

the square root of the kinetic constant k of the chemical reaction and thus quantifies the coupling strength between the hydrodynamic motions and the RD processes. In a previous study [16], we explored the characteristics of the dynamics as a function of M keeping the height of the layer L_z fixed. Considering the definition of the dimensionless Marangoni number (13), we see that analyzing the corresponding changes of M is rather difficult to do in experiments as it implies changing the reaction or the chemical species (to change D, the kinetic constant k or $d\gamma/dc$) or to vary the viscosity of the solvent μ hoping that this will not affect $d\gamma/dc$. It is much more easy to consider an experiment in which stocks of reactant solutions are prepared once and for all for which the variation of Marangoni flows is studied by varying the thickness of the solution layers in a Petri dish. To predict what is to be expected in that case, the goal of the present paper is to fix M and study the influence of a variable L_z on the dynamics.

To do so, we numerically integrate Eqs. 6–8 by finite-difference methods [16]. The initial condition corresponds to a planar RD front propagating in the solution in the absence of any fluid flow. Hence, the initial fluid velocity and the hydrostatic pressure gradient are set to zero, while the initial RD profile for the concentration of the surface-active product c is taken to follow the analytical solution

$$c(x, t) = \frac{1}{1 + e^{(x-vt)/\sqrt{2}}} = \frac{1}{2}\left[1 + \tanh\left(-\frac{\sqrt{2}}{4}(x - vt)\right)\right], \tag{14}$$

where $v = \sqrt{2}/2$ is the constant RD speed of the front. This profile is the solution of Eqs. 6–8 with $\underline{v} = 0$ corresponding to the kinetically stable chemical-product steady state $c = 1$ invading the $c = 0$ marginally stable reactant solution [5,18,19]. The width w_{RD} of this front, arbitrarily defined here as the distance between $c = 0.01$ and $c = 0.99$, equals $w_{RD} = 2\sqrt{2}\log 99 = 13$. This definition allows for an easy study of the deformation of the front by Marangoni flows in the depth of the layer by a simple tracking of the $c = 0.01$ and $c = 0.99$ isoconcentration lines.

3 Influence of the solution-layer thickness on chemically induced Marangoni convection

We have shown in a previous study [16] that fixing the layer thickness to $L_z = 10$ and varying the Marangoni number M leads to increased deformation of the front by capillary flows and that the asymptotic dynamics is a steady vortex traveling with the front at a non-linear speed V which is an increasing function of M. As explained above, it is, however, simpler experimentally to keep M fixed and vary L_z. In order to predict the changes of spatio-temporal dynamics of the RDC system in that case, we fix here M to a typical value of 100 throughout the rest of the paper and analyze the influence of variations of L_z ($4.0 \leq L_z \leq 30.0$). As a reference situation, we start in Fig. 2 with a layer of thickness $L_z = 10$, i.e., a height comparable to the width of the chemical front. This would correspond to a rather thin layer of the order of one millimeter in thickness, which is the typical magnitude of the RD width of a chemical front [5]. Because of the concentration gradient across the front, capillary flows generated at the solution–air interface (see boundary condition (12)) accelerate the front to the right at the surface, inducing a deformation of the front across the layer. After a given transient, the deformation saturates and the system evolves towards a steady vortex. This vortex stretches the chemical front which has a larger width than the RD width w_{RD} and travels at a non-linear speed V larger than the RD speed v because of the presence of convection.

As the layer thickness L_z is increased for a fixed M, the acceleration at the surface is initially the same, as the concentration gradient across the pure RD front is the same. Nevertheless, as the flow has a larger thickness in which to develop, the system takes a longer time to reach an asymptotic dynamics and the stretching of the front at the surface is of increased amplitude. This can be seen by comparing Figs. 2 and 3 which correspond to the spatio-temporal dynamics of the concentration c shown at the same successive times for $L_z = 10$ and $L_z = 20$, respectively. For $L_z = 10$, the system needs roughly $25\tau_c$ to reach an asymptotic steady convective roll traveling with the front and deforming it while $35\tau_c$ are needed to reach a similar dynamics for $L_z = 20$. In both Figs. 2 and 3, it can be appreciated that, during the transient needed to reach that asymptotic dynamics, the front is immediately

Fig. 2 Deformation of a
chemical front by
Marangoni effects for
$M = 100$, and $L_z = 10$
shown from top to bottom
from $t = 0$ up to $t = 60$
with a time interval of
$\Delta t = 5$. The aspect ratio
between x and z directions
is preserved
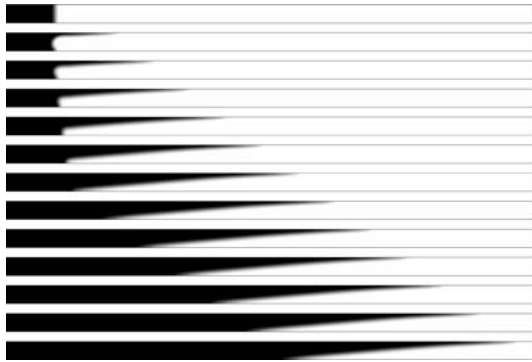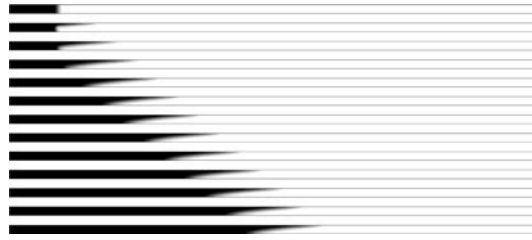
Fig. 3 Deformation of a chemical front by Marangoni effects
for $L_z = 20$. All other parameters are as in Fig. 2
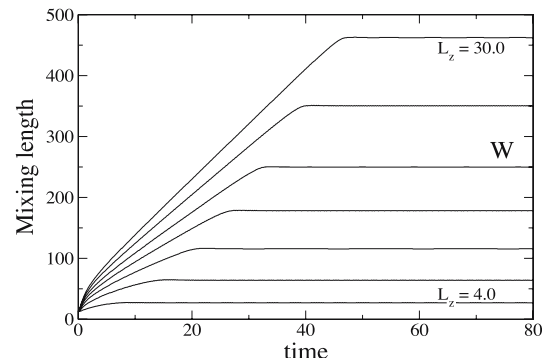
Fig. 4 Temporal evolution of the mixing length for various
values of the layer thickness, $L_z = 4; 8; 12; 16; 20; 25; 30$
from bottom to top

strongly deformed at the surface by Marangoni flows and very soon reaches the RDC speed V. On the contrary, at the bottom of the layer, the front travels at the RD speed v during the time necessary for the convection initiated at the surface to cross the layer. This effect can be correlated to the temporal evolution of the mixing length defined as the distance between $\bar{c} = 0.01$ and $\bar{c} = 0.99$, where $\bar{c}(x, t)$ is the concentration profile averaged along the thickness of the layer [16]. This distance typically characterizes the deformation of the front across the layer which increases as long as there is a difference of propagation speed between the front at the top and at the bottom of the layer. Indeed, as can be seen in Fig. 4, the mixing length initially increases rapidly and after that linearly, this latter trend corresponding to the convective transport of the surface acceleration towards the bulk. When chemical reaction, diffusion and convection finally balance, the system reaches a saturated deformation characterized by a constant mixing length. The corresponding steady vortex and front deformation express the reach of a balance between two competitive effects: Marangoni flows stretch the front, smoothing out in turn the concentration gradients that drive them. In Fig. 5, we plot the constant asymptotic value W of the mixing length as a function of L_z, noting that W is an increasing function of L_z. Similarly, the non-linear RDC speed V increases with the layer thickness L_z as can be seen in Fig. 6.
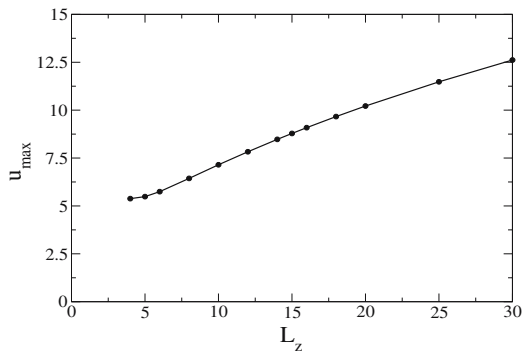
To characterize the asymptotic velocity field, we analyze the maximum absolute value of the horizontal component u as a function of L_z (Fig. 7). This maximum value is always positive and directed towards the reactants at the surface. Its amplitude increases with the layer thickness L_z, probably due to the fact that the system is less influenced by the no-slip boundary condition at the bottom when L_z increases. Figure 8 shows the asymptotic profiles of the horizontal component u across the layer plotted as a function of the renormalized height and taken at the position along x where $|u|$ is maximum for the various L_z. The maximum and minimum values of u are located, respectively, at the surface and at roughly $L_z/3$ for all the values of L_z we have screened, while the flow changes its direction around $z = 2L_z/3$.
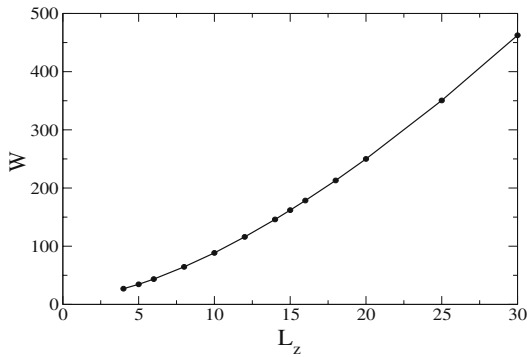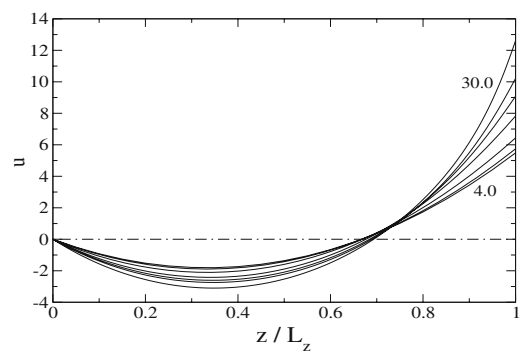
Fig. 5 Asymptotic mixing length W as a function of the layer thickness L_z
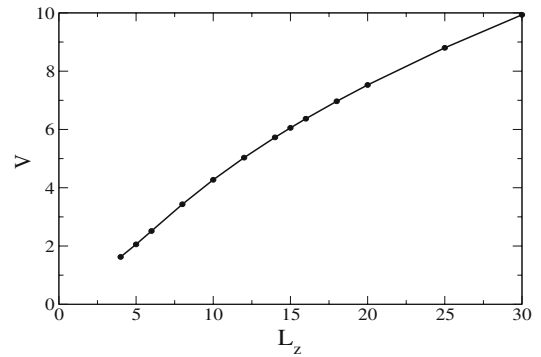
Fig. 6 Non-linear reaction–diffusion–convection speed V as a function of the layer thickness L_z

Fig. 7 Maximum value of the horizontal component of the asymptotic velocity field, $u_{\max}$, as a function of the layer thickness L_z

Fig. 8 Horizontal component of the asymptotic fluid flow, u, taken at $x = x_{|u|=|u|_{\max}}$ along the renormalized height of the layer for various values of the layer thickness, $L_z = 4; 8; 12; 16; 20; 25; 30$

4 Conclusions

Chemical fronts traveling in solution layers in contact with air can be accelerated and deformed because of the presence of Marangoni flows if one of the chemical species involved in the reaction is surface-active. We have analyzed here numerically the influence of the thickness of the solution layer on the asymptotic non-linear dynamics resulting from such a coupling between hydrodynamic capillary flows and RD processes in the absence of gravity. Fixing the Marangoni number to a constant value, we have varied the layer thickness L_z to show that increasing flows result. The asymptotic dynamics is a steady vortex traveling at a constant speed V larger than the RD speed and deforming the front. This steady dynamics is reached sooner for smaller L_z and is a compromise between RD processes which provide the sharp chemical front at the origin of the surface-tension gradients and Marangoni flows which tend to smooth out and thus kill those gradients.

Numerous experimental evidences of front deformations induced by Marangoni effects exist in the literature. Careful quantitative experimental studies of the asymptotic dynamics need, however, still to be performed to allow for precise comparison with the present theoretical analysis.

From a theoretical point of view, this work also calls for further extensions. The present study has been performed for a fixed positive Marangoni number assuming that the product of the reaction is decreasing the surface tension of the liquid solvent. In that case, the front propagates in the same direction as that of the Marangoni flows generated

at the liquid–air interface. A similar study could be performed in the future for a negative Marangoni number for which the direction of the capillary flow initiated at the surface is opposite to that of the front. Further studies should also address the possible influence of pure buoyancy-driven flows in a similar geometry before tackling the complicated possible influence of both density-driven and surface-tension-driven flows on the propagation properties of chemical fronts. Let us also mention that the current study has neglected possible deformation of the interface as well as thermo-capillary effects that could be driven by the exothermicity of the reaction. Such extensions might be a topic for future theoretical research.

References

1. De Wit A (2004) Miscible density fingering of chemical fronts in porous media: nonlinear simulations. Phys Fluids 16(1):163–175
2. Böckmann M, Müller SC (2004) Coarsening in the buoyancy-driven instability of a reaction-diffusion front. Phys Rev E 70(4):046302
3. Bánsági T Jr, Horváth D, Tóth Á (2004) Nonlinear interactions in the density fingering of an acidity front. J Chem Phys 121(23):11912–11915
4. Gribschaw TA, Showalter K, Banville DL, Epstein IR (1981) Chemical waves in the acidic iodate oxidation of arsenite. J Phys Chem 85:2152–2155
5. Hanna A, Saul A, Showalter K (1982) Detailed studies of propagating fronts in the iodate oxidation of arsenous acid. J Am Chem Soc 104:3838–3844
6. Bazsa G, Epstein IR (1985) Traveling waves in the nitric acid-iron(II) reaction. J Phys Chem 89:3050–3053
7. Pojman JA, Epstein IR (1990) Convective effects on chemical waves: 1. Mechanisms and stability criteria. J Phys Chem 94:4966–4972
8. Miike H, Yamamoto H, Kai S, Müller SC (1993) Accelerating chemical waves accompanied by traveling hydrodynamic motion and surface deformation. Phys Rev E 48:1627–1630
9. Kai S, Miike H (1994) Hydrochemical soliton due to thermocapillary instability in Belousov–Zhabotinsky reaction. Physica A 204:346–358
10. Kai S, Ariyoshi T, Inanaga S, Miike H (1995) Curious properties of soliton induced by Marangoni instability in shallow Belousov–Zhabotinsky reaction. Physica D 84(1–2):269–275
11. Inomoto O, Ariyoshi T, Inanaga S, Kai S (1995) Depth dependence of the big wave in Belousov–Zhabotinsky reaction. J Phys Soc Jpn 64(10):3602–3605
12. Inomoto O, Kai S, Ariyoshi T, Inanaga S (1997) Hydrodynamical effects of chemical waves in quasi-two-dimensional solution in Belousov–Zhabotinsky reaction. Int J Bif Chaos 7(5):989–996
13. Hauser MJB, Simoyi RH (1994) Inhomogeneous precipitation patterns in a chemical wave. Phys Lett A 191(1–2):31–38
14. Martincigh BS, Simoyi RH (1995) Convective instabilities induced by an exothermic autocatalytic chemical reaction. Phys Rev E 52(2):1606–1613
15. Martincigh BS, Simoyi RH (2002) Pattern formation fueled by dissipation of chemical energy: conclusive evidence for the formation of a convective torus. J Phys Chem A 106(3):482–489
16. Rongy L, De Wit A (2006) Steady Marangoni flow traveling with chemical fronts. J Chem Phys 124:164705
17. Nepomnyashchy AA, Velarde MG, Colinet P (2002) Interfacial phenomena and convection. Chapman and Hall/CRC, Boca Raton
18. Merkin JH, Ševčiková H (1999) Travelling waves in the iodate–arsenous acid system. Phys Chem Chem Phys 1:91–97
19. Field RJ, Burger M (eds) (1985) Oscillations and traveling waves in chemical systems. Wiley, New York